Journal of Sound and Vibration (2001) **242**(2), 369–376
doi:10.1006/jsvi.2000.3331, available online at http://www.idealibrary.com on IDEAL®

SOUND TRANSMISSION IN CIRCULAR DUCTS OF CONTINUOUSLY VARYING CROSS-SECTIONAL AREA

M. Utsumi

Machine Element Department, Technical Research Laboratory, Ishikawajima-Harima Heavy Industries Company Ltd. (IHI), 3-1-15 Toyosu, Koto-ku, Tokyo 135-8732, Japan.
E-mail: masahiko_utsumi@ihi.co.jp

(*Received* 13 *September* 2000)

1. INTRODUCTION

The study of the reflection and transmission coefficients of acoustic waves in ducts of continuously varying cross-sectional area has been of interest to many researchers in the past. Thus, various numerical methods for predicting these coefficients have been developed, such as the method of weighted residuals [1–3], the finite element method [4, 5], the perturbation method [6, 7], the boundary element method [8], and the matricial Riccati equation method [9]. Another approach adopted by several researchers [10–12] is to represent a non-uniform duct with a series of stepped uniform ducts and systematically account for the reflection and transmission process which occurs at each intersection of the stepped elements. These conventional methods require an iterative calculation or solution of a very high-dimensional numerical problem due to the segmentation of the duct into many subsections. In the author's previous paper [13], a more efficient analytical method was presented, which requires neither segmentation nor iterative calculation. In this method, spherical co-ordinates were introduced according to the geometry of the non-uniform section of the duct, thereby determining analytically a system of characteristic functions for various profiles of the non-uniform portion.

The present study is an extension of the previous work. The new points of the present paper are as follows:

(1) A more efficient formulation based on a variational principle is presented.
(2) A numerical computation is carried out for the case in which a slight change of the duct profile is helpful in applying the present method. The previous paper pointed out such a case, but did not present numerical examples for it.

2. METHOD OF SOLUTION

The system model to be considered is shown in Figure 1. Two semi-infinite uniform duct sections are joined by a non-uniform transition section of length L. For all sections, the side wall of the duct is assumed to be rigid. The cylindrical co-ordinates r, φ and z are used to express the solution in the uniform sections $z \leqslant 0$ and $L \leqslant z$, while the spherical co-ordinates R, θ and φ are introduced to determine analytically the characteristic functions for the non-uniform portion $0 \leqslant z \leqslant L$. The origin O of the spherical co-ordinates is chosen

0022-460X/01/170369 + 08 $35.00/0 © 2001 Academic Press

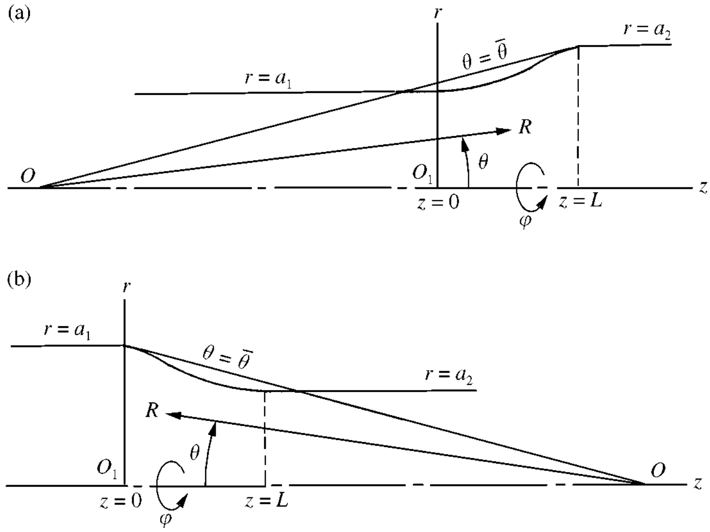

Figure 1. Computational model and co-ordinate systems (diverging (a) and converging (b) tapered transition sections).

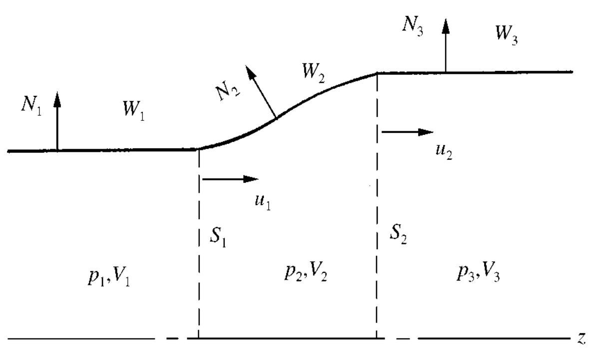

Figure 2. Diagram of duct and symbols.

as the apex of a cone having a side wall tangent to the duct wall at the largest cross-section.

To derive the governing equations in terms of a weighted-integral form, a variational principle is introduced. Considering harmonic motion of the form $e^{i\omega t}$, the variational principle can be expressed as

$$\delta \sum_{i=1}^{3} \iiint_{V_i} \tfrac{1}{2}[(\nabla p_i)^2 - k^2 p_i^2] \mathrm{d}V_i + \delta \iint_{S_1} (p_2 - p_1)\rho\omega^2 u_1 \, \mathrm{d}S_1 + \delta \iint_{S_2} (p_3 - p_2)\rho\omega^2 u_2 \, \mathrm{d}S_2 = 0, \tag{1}$$

where V_1, V_2 and V_3 are the domains within the range $z \leqslant 0$, $0 \leqslant z \leqslant L$ and $z \geqslant L$, respectively, as shown in Figure 2, S_i is the interface between V_i and V_{i+1}, p_i is the sound pressures in the domain V_i, u_i is the fluid particle displacement in the z direction on the surface S_i, k is the wave number, ρ is the fluid density, and ω is the angular frequency of interest. The wave number k is given by

$$k = \omega/c, \tag{2}$$

where c is the speed of sound. By using Green's theorem and the momentum equation $\rho\omega^2 u_i = \partial p_i/\partial z$, equation (1) can be transformed into

$$\begin{aligned} &-\sum_{i=1}^{3}\iiint_{V_i}(\nabla^2 p_i + k^2 p_i)\delta p_i \, \mathrm{d}V_i \\ &+\int_0^{2\pi}\int_0^{a_1}\left\{\left(\frac{\partial p_1}{\partial z} - \frac{\partial p_2}{\partial z}\right)\delta p_2 - (p_1 - p_2)\frac{\partial(\delta p_1)}{\partial z}\right\}\bigg|_{z=0} r\,\mathrm{d}r\,\mathrm{d}\varphi \\ &+\int_0^{2\pi}\int_0^{a_2}\left\{\left(\frac{\partial p_2}{\partial z} - \frac{\partial p_3}{\partial z}\right)\delta p_3 - (p_2 - p_3)\frac{\partial(\delta p_2)}{\partial z}\right\}\bigg|_{z=L} r\,\mathrm{d}r\,\mathrm{d}\varphi \\ &+\sum_{i=1}^{3}\iint_{W_i}\frac{\partial p_i}{\partial N_i}\delta p_i \, \mathrm{d}W_i = 0, \end{aligned} \tag{3}$$

where N_i represents the outward normal of the duct wall W_i (Figure 2). Equation (3) yields the following governing equations:

$$\nabla^2 p_i + k^2 p_i = 0 \quad \text{in } V_i \quad (i = 1, 2, 3), \tag{4}$$

$$p_1 = p_2, \quad \frac{\partial p_1}{\partial z} = \frac{\partial p_2}{\partial z} \quad \text{on } z = 0, \tag{5}$$

$$p_2 = p_3, \quad \frac{\partial p_2}{\partial z} = \frac{\partial p_3}{\partial z} \quad \text{on } z = L, \tag{6}$$

$$\frac{\partial p_i}{\partial N_i} = 0 \quad \text{on } W_i \quad (i = 1, 2, 3). \tag{7}$$

Equation (4) represents the wave equation in each domain. Equations (5) and (6) indicate that the sound pressure and the fluid particle velocity are continuous at the interfaces between the uniform and non-uniform portions. Equation (7) corresponds to the condition that the fluid particle velocity in the direction normal to the rigid duct wall vanishes.

In the subsequent analysis, we first determine admissible functions for the sound pressures p_1, p_2 and p_3 by solving the wave equation analytically. We then use the Galerkin method to transform the variational principle (3) into algebraic linear equations that are solved to determine the reflection and transmission coefficients.

Applying the cylindrical co-ordinates as shown in Figure 1 to equations (4) and (7) for $i = 1$ and 3, the admissible functions for p_1 and p_3 can be expressed as

$$\begin{aligned} p_1 = {} & \left[C_{1mv}\mathrm{J}_m(\mu_{1mv}r)\exp(-\mathrm{i}k_{1mv}z) + \sum_{n=n_{min}}^{n_{max}} C_{2mn}\mathrm{J}_m(\mu_{1mn}r)\exp(\mathrm{i}k_{1mn}z)\right] \\ & \times \cos m\varphi \exp(\mathrm{i}\omega t), \end{aligned} \tag{8}$$

$$p_3 = \sum_{n=n_{min}}^{n_{max}} C_{3mn}\mathrm{J}_m(\mu_{2mn}r)\exp[-\mathrm{i}k_{2mn}(z - L)]\cos m\varphi \exp(\mathrm{i}\omega t) \tag{9}$$

with

$$(k_{1mn})^2 = [\omega^2 - (c\mu_{1mn})^2]/c^2 \quad (k_{2mn})^2 = [\omega^2 - (c\mu_{2mn})^2]/c^2, \tag{10}$$

$$n_{min} = 0 \quad (\text{for } m = 0), \quad n_{min} = 1 \quad (\text{for } m \geqslant 1), \tag{11}$$

where C_{1mv}, C_{2mn} and C_{3mn} are complex constants, J_m is the Bessel function of the first kind of order m, and μ_{1mn} and μ_{2mn} are the nth roots of $J'_m(\mu a_1) = 0$ and $J'_m(\mu a_2) = 0$ respectively. Note that the constants $\mu_{100} = \mu_{200} = 0$ are defined such that equations (8) and (9) include the plane wave mode having a constant sound pressure distribution throughout the cross-section of the duct.

In equations (8) and (9), C_{1mv}, C_{2mn} and C_{3mn} represent the incident, reflected and transmitted waves respectively. Since the purpose here is to determine the reflection and transmission coefficients for a prescribed mode (m, v) of the incident wave, the incident wave is expressed in terms of the mode (m, v) alone. The summation over n in equations (8) and (9) can be physically explained by the fact that the divergence or convergence, under a modal excitation with mode (m, v), will generate reflections and transmissions following a series of radial modes having the same circumferential wave number m. A summation for m is not necessary here, since the three sections, $z \leqslant 0$, $0 \leqslant z \leqslant L$ and $L \leqslant z$, are coaxial. This method can be applied to non-coaxial cases by using admissible functions expressed in terms of a series of circumferential modes.

Expressing equation (4) for $i = 2$ in terms of the spherical co-ordinates shown by Figure 1 and solving the resulting equation leads to [13]

$$p_2 = \sum_{n=n_{min}}^{n_{max}} \sum_{l=1}^{2} A_{mnl} F_{mnl}(R) \Theta_{mn}(\theta) \cos m\varphi \mathrm{e}^{\mathrm{i}\omega t} \tag{12}$$

with

$$F_{mn1}(R) = (kR)^{-1/2} \mathrm{J}_{\sqrt{\lambda + 0{\cdot}25}}(kR), \quad F_{mn2}(R) = (kR)^{-1/2} \mathrm{J}_{-\sqrt{\lambda + 0{\cdot}25}}(kR), \tag{13}$$

$$\Theta_{mn}(\theta) = \sin^m \theta F_{GAUSS}(m - \alpha, \alpha + m + 1, m + 1, (1 - \cos\theta)/2), \tag{14}$$

where F_{GAUSS} denotes the Gaussian hypergeometric series, λ is the characteristic value, and α is a parameter determined by $\alpha(\alpha + 1) = \lambda$. The characteristic value λ is determined such that solution (14) satisfies the boundary condition

$$\frac{\mathrm{d}\Theta}{\mathrm{d}\theta} = 0 \quad \text{at } \theta = \bar{\theta}. \tag{15}$$

Substituting the admissible functions (8), (9) and (12) into equation (3) and considering the variation with respect to C_{1mv}, C_{2mn}, C_{3mn} and A_{mnl} leads to a system of algebraic linear homogeneous equations for the generalized co-ordinates C_{1mv}, C_{2mn}, C_{3mn} and A_{mnl}. By solving this system of equations, we can determine the following reflection coefficient R_{mv} and transmission coefficient T_{mv} for a specified incident mode (m, v):

$$R_{mv} = |C_{2mv}/C_{1mv}|, \quad T_{mv} = |C_{3mv}/C_{1mv}|. \tag{16}$$

In the previous paper [13], the boundary conditions were derived through physical intuition and then the conventional Fourier–Bessel expansion technique was used to derive algebraic equations with respect to the generalized co-ordinates. As a result, it was necessary to treat the diverging and converging cases separately (see pp. 741–742 in reference [13]). In the present study, on the other hand, the combined and integrated form (3) of the governing equations based on the variational principle (1) requires only a routine substitution of the admissible functions (8), (9) and (12) into equation (3) to obtain algebraic equations for the generalized co-ordinates.

3. NUMERICAL EXAMPLES

To verify the present analysis, numerical computation was carried out for identical cases given in the previous paper [13]. The results obtained from the present analysis completely agree with those shown in Figures 4 and 5 in the previous paper. For brevity, these figures are not presented here.

Numerical calculation is conducted for the case in which a slight change of the duct profile effects the use of the spherical co-ordinates (for details, see p. 740 of the previous paper [13]). Figure 3 shows the geometry of the transition section employed as a numerical example. Only the diverging transition section is shown, because the converging transition section is exactly the reverse of the diverging one. The geometry of the diverging transition section is determined by

$$r = r_W(z) = Az^2 + Bz + C \quad (0 \leqslant z \leqslant L), \tag{17}$$

where the constants A, B and C are determined such that $r_W|_{z=0} = a_1 = 0{\cdot}021$ m, $r_W|_{z=L} = a_2 = 0{\cdot}03$ m, and $\mathrm{d}r_W/\mathrm{d}z|_{z=0} = 0{\cdot}2(a_2 - a_1)/L$ ($L = 0{\cdot}015$ m).

Figures 4 and 5 show the solutions for the diverging and converging tapered transition sections respectively. These results are shown within the frequency range $\omega > \max(c\mu_{1mv}, c\mu_{2mv})$, in which the mode (m, v) is an advancing wave in all portions of the duct, and hence extremely useful in engineering applications. Below this frequency domain, the mode (m, v) does not propagate since both or either of the wave numbers k_{1mv} and k_{2mv} is a pure imaginary number, as can be seen from equation (10).

To verify the numerical results, numerical computation was carried out according to a conventional method that represents the non-uniform section with a series of stepped

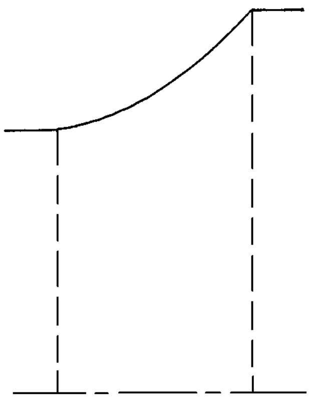

Figure 3. Profile of transition section employed as numerical example (only the diverging case is shown; the converging case is exactly the reverse of the diverging one).

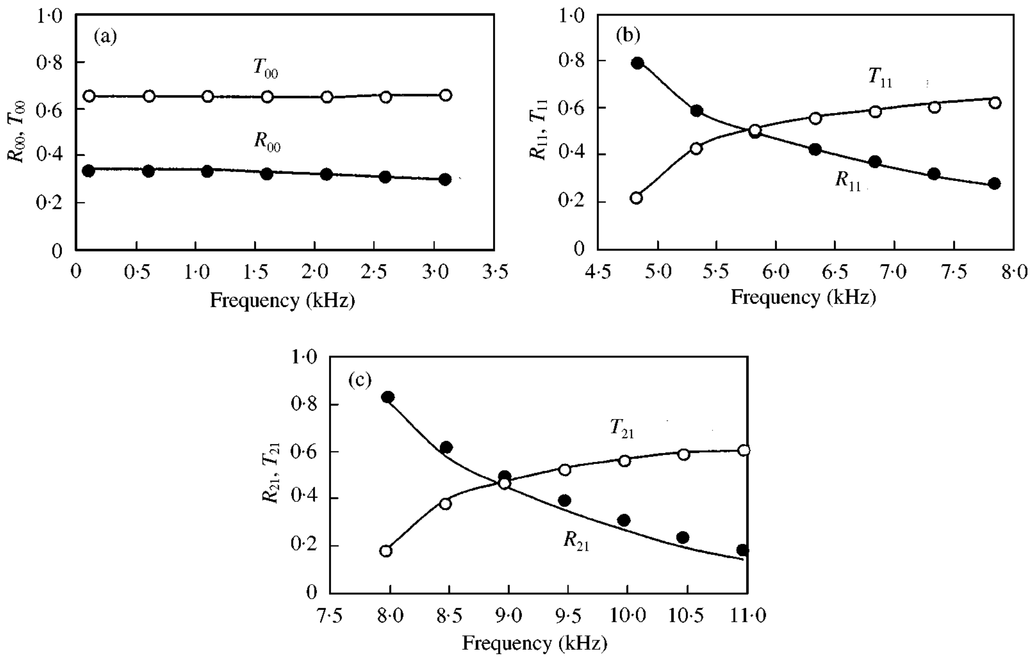

Figure 4. Reflection coefficient $R_{m\nu}$ and transmission coefficient $T_{m\nu}$ for diverging tapered transition section shown in Figure 3: ——, present method; • and ○, conventional method; (a) incident mode $(m, \nu) = (0, 0)$, (b) incident mode $(m, \nu) = (1, 1)$, (c) incident mode $(m, \nu) = (2, 1)$.

uniform ducts and applies the method described in reference [14]. The number of the elements is 10. The result obtained by the conventional method are marked in Figures 4 and 5. Acceptable agreement can be confirmed between the results obtained by the present analysis and those of the conventional theoretical prediction.

4. CONCLUSION

A method of solution based on a variational principle has been presented in this paper for the acoustic wave propagation in ducts having a continuous change in cross-sectional area. This method is more efficient than the previous approach [13] using the conventional Fourier–Bessel expansion technique, because the present method requires only a routine substitution of the admissible functions into the combined and integrated form of the governing equations for obtaining linear algebraic equations for the generalized co-ordinates. The numerical results obtained by the present method are in good agreement with the solutions given in the previous paper [13].

A numerical study in this paper addressed the case in which a slight change of the duct profile is helpful to effect the use of the proposed analytical approach. As a verification of the numerical results, these are compared with the results obtained by a conventional method that approximates the cross-sectional area variations as a series of stepwise expansions and contractions, and applies the method described in reference [14]. Acceptable agreement was confirmed between the results from the present and the conventional methods.

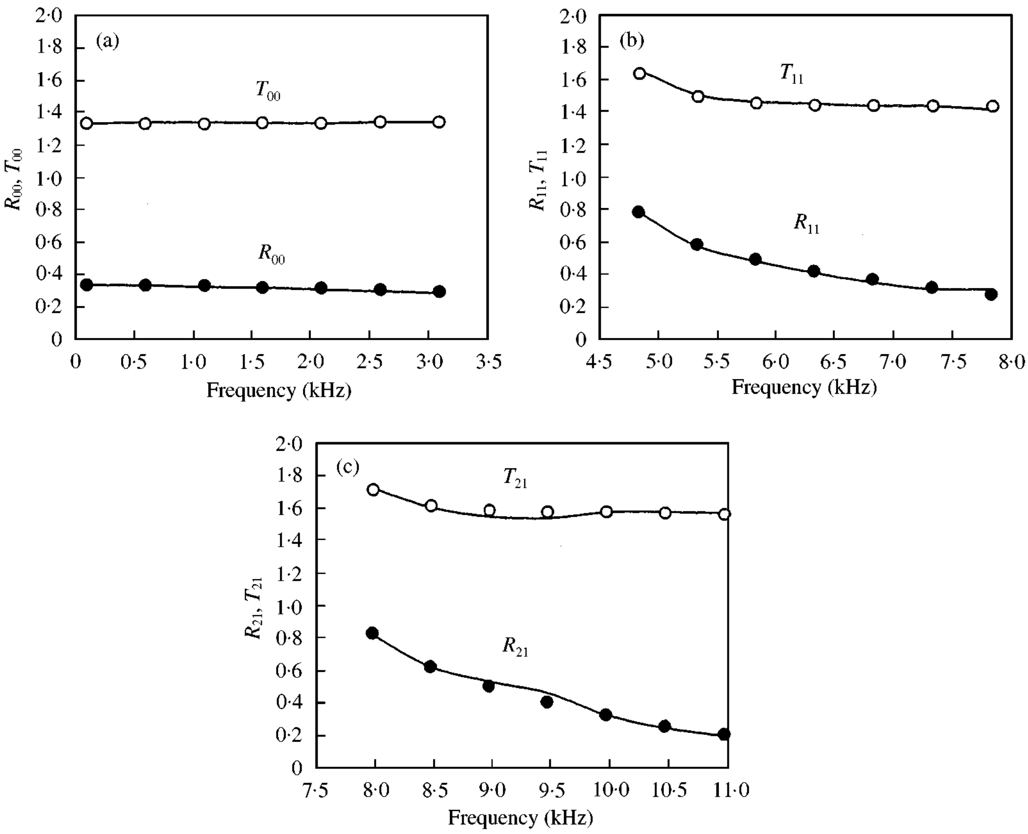

Figure 5. Reflection coefficient $R_{m\nu}$ and transmission coefficient $T_{m\nu}$ for converging tapered transition section which is exactly the reverse of the diverging one: ——, present method; ● and ○, conventional method; (a) incident mode $(m, \nu) = (0, 0)$, (b) incident mode $(m, \nu) = (1, 1)$, (c) incident mode $(m, \nu) = (2, 1)$.

REFERENCES

1. W. Eversman, E. L. Cook and R. J. Beckemeyer 1975 *Journal of Sound and Vibration* **38**, 105–123. A method of weighted residuals for the investigation of sound transmission in non-uniform ducts without flow.
2. P. T. Vo and W. Eversman 1978 *Journal of Sound and Vibration* **56**, 243–250. A method of weighted residuals with trigonometric basis functions for sound transmission in circular ducts.
3. W. Eversman and R. J. Astley 1981 *Journal of Sound and Vibration* **74**, 89–101. Acoustic transmission in non-uniform ducts with mean flow. Part I: the method of weighted residuals.
4. R. J. Astley and W. Eversman 1978 *Journal of Sound and Vibration* **57**, 367–388. A finite element method for transmission in non-uniform ducts without flow: comparison with the method of weighted residuals.
5. R. J. Astley and W. Eversman 1981 *Journal of Sound and Vibration* **74**, 103–121. Acoustic transmission in non-uniform ducts with mean flow. Part II: the finite element method.
6 A. H. Nayfeh, J. E. Kaiser, R. L. Marshall and C. J. Hurst 1980 *Journal of Sound and Vibration* **71**, 241–259. A comparison of experiment and theory for sound propagation in variable area ducts.
7. C. K. W. Tam 1971 *Journal of Sound and Vibration* **18**, 339–351. Transmission of spinning acoustic modes in a slightly non-uniform duct.
8. A. D. Sahasrabudhe, M. L. Munjal and R. S. Anantha 1992 *Noise Control Engineering Journal* **38**, 27–38. Design of expansion chamber mufflers incorporating 3-D effects.

9. V. Pagneux, N. Amir and J. Kergomard 1996 *Journal of the Acoustical Society of America* **100**, 2034–2048. A study of wave propagation in varying cross-section waveguides by modal decomposition. Part I. Theory and validation.
10. W. E. Zorumski and L. R. Clark 1971 *Unpublished working paper*, *NASA Langley Research Center*. Sound radiation from a source in an acoustically treated circular duct.
11. R. J. Alfredson 1972 *Journal of Sound and Vibration* **23**, 433–442. The propagation of sound in a circular duct of continuously varying cross-sectional area.
12. A. Sadamoto, Y. Murakami and S. Masuda 1993 *Journal of Acoustical Society of Japan* **49**, 235–242. Calculation for reflection and transmission of higher-order mode sound waves at sections of varying cross-sectional area in circular ducts (in Japanese).
13. M. Utsumi 1999 *Journal of Sound and Vibration* **227**, 735–748. An efficient method for sound transmission in non-uniform circular ducts.
14. J. Miles 1944 *Journal of the Acoustical Society of America* **16**, 14–19. The reflection of sound due to a change in cross section of a circular tube.